Proceedings of the 3rd International Conference on Computing Innovation and Applied Physics
DOI: 10.54254/2753-8818/14/20240944

Integrated L1 adaptive cartesian PD control for robotic loco-manipulation

Muqun Hu

Department of Aerospace and Mechanical Engineering, University of Southern California, Los Angeles, USA

muqunhu@alumni.usc.edu

Abstract. This paper presents an integrated framework of L1 adaptive control and Cartesian PD control that overcomes the inherent limitations of the latter controller in tracking end effector position for loco-manipulation tasks. In a simplified system, this work represented the loco-manipulation problem with the Cartesian space dynamics of the end effector object, capturing the dominating parts of the dynamics in linear terms. The unmodeled nonlinear dynamics, along with other model uncertainties and external disturbances, are accounted for by the L1 adaptive controller, taking the Cartesian PD input as a component of the control law to resemble its behavior for the desired system dynamics modeled in the state predictor of the L1 adaptive controller. Through simulation results of various combinations of model perturbations and external disturbances, we show that this integrated framework can achieve similar tracking performances of the end effector and object without the need to re-tune controller parameters. This work demonstrated the mitigation of effects from system uncertainties with model perturbation of up to 100% higher than expected mass and up to 15N of sinusoidal external disturbances, with higher disturbance rejection possible through designing for more conservative estimates of unknown model parameters. Combined with the low computational cost of this framework, the improvement in state command tracking gives rise to potential implementation on robotic systems controlled with linear optimization formulations.

Keywords: Adaptive Control, Loco-Manipulation, Robotics, State Space Representation.

1. Introduction

In the past few years, mounting a manipulator to a floating base became a common solution for the need to manipulate objects at a variety of locations. Some common designs for such solution are arm mounted quadruped robots. In these designs, the quadruped robot has the ability to maneuver to a wide range of positions, both relative to the object for manipulation and in the operating environment; meanwhile, the arm enables the system to exert forces on the object in directions that are not only aligned with the robot's direction of travel. Although transporting the robot between positions (locomotion) and moving objects with an arm (manipulation) are well explored, such as utilizing model predictive control (MPC) for optimization in [1-3], performing those tasks simultaneously is not trivial. Hence, a new type of control problem emerged – loco-manipulation – which operates or transports an object with the manipulator while the floating base moves to a different position. Two challenges are posed as a result of the coupling dynamics of the floating base and the manipulator: the dynamic forces of manipulation

DOI: 10.54254/2753-8818/14/20240944

affecting the stability of locomotion and the oscillations and tracking error of locomotion reducing the precision and accuracy of manipulation tasks.

This framework will primarily address the latter of the issues, focusing on improvements of manipulator end effector tracking. While performing loco-manipulation tasks, the quadruped robot often employs a stepping or trotting gait, resulting in phases of only 2 ground contact points, frequently causing oscillations in the rotational and translational position and velocities of the robot body, in addition to the impact on the robot dynamics from external disturbances. Further, the dynamics of the arm are nonlinear, especially when the end effector is not fully independent from the robot body in the six degrees of freedom (DOF) of a rigid body. In order to mitigate the effects of the nonlinear dynamics on end effector tracking, recently introduced frameworks utilized nonlinear MPC and whole-body control in order to capture the nonlinearity on robot-object dynamics and optimize for desired robot and object states and inputs, which is shown to be computationally heavy and require state-of-the-art processors to implement on-board [4]. This work introduces a framework based on classical control and requires minimal computational resources.

Compared to common approaches of designing a PD controller in joint space, Cartesian PD control conveniently expresses the linear components of the object dynamics and receives command in Cartesian space, without the need of performing inverse-kinematics for different configurations of the arm. Further, the expression of dynamics on Cartesian space allows easy tuning and linear analysis of the PD controller for the object dynamics. However, PD controllers are inherently subject to steady state error due to external disturbances, while one can add an integrator to eliminate steady state error, gain tuning would be specific to the model inertia and damping properties, easily leading to unacceptable transient errors and instability with large model perturbations.

L1 adaptive control has been shown to maintain its robustness with fast adaptation for uncertainties within a certain bandwidth, while keeping the transient error bounded [5]. Having been demonstrated on a variety of aerospace and mechanical systems, especially in safety-critical ones in aircraft flight testing [6], L1 adaptive control is suitable for implementation on loco-manipulation tasks, being able to capture perturbations in the object inertial properties and external reaction forces quickly, reducing the tracking error of end effector trajectories. It is important for the adaptation law to be able to quickly mitigate a wide range of uncertainties, both matched and unmatched, without losing robustness compared to conventional model reference adaptive control (MRAC) [7, 8]. While physical perturbations and disturbances related to loco-manipulation tasks can often be bounded within a certain frequency, designing the bandwidth of the filter for L1 adaptive control in this application is straightforward, allowing room for trade-off between transient performance and time-delay margin [9]. Hence, by integrating L1 adaptive control with Cartesian PD control, this research found out that the tracking error of the end effector position for a manipulator on a floating base can be mitigated, without the need of re-tuning either component of the controller, while utilizing minimal computational performance [10]. A simplified model of a 1 DOF floating base and a 1 DOF manipulator was used in this work, allowing end effector tracking in 2D space. The results of this work demonstrated the potential for such framework to be integrated with linear optimal control methods such as quadratic programming, previously demonstrated with general applications for robotic systems [11].

The rest of the paper is organized as follows. Section 2 introduces the design and relevant proofs for extension of the Cartesian PD and L1 adaptive controller, as well as the integrated framework. Section 3 presents numerical simulation results of the system subjected to various uncertainties, showing the performance improvement by the integrated L1 adaptive Cartesian PD controller. Section 4 concludes the findings and discusses potential directions of improvement and further work.

2. Control System Framework

2.1. Simplified Model

To directly and clearly show the effectiveness of the integrated L1 adaptive Cartesian PD controller, this work used a simplified model of a robot body with a 1 DOF arm. The robot base has 1 DOF movement

DOI: 10.54254/2753-8818/14/20240944

in the horizontal (x) direction, while the arm rotates in the axis (y) orthogonal to the direction of the base movement and the world vertical axis (z). This creates a 2D space in the xz plane for the end effector, representing a minimally simplified range of motion for common manipulation tasks. The robot base is actuated in the direction of travel, representing the dynamic locomotion force; the 1 DOF arm is actuated with a torque input, simulating the torque required to achieve object manipulation and end effector tracking.

Considering the two degrees of freedom of actuation – the position of the moving base x_b and the angle of the arm θ – the nonlinear dynamics of the system can be written as

$$\begin{bmatrix} m_{\mathrm{b}} + m_{\mathrm{a}} + m_{\mathrm{o}} & -\left(\frac{m_a}{l_{\mathrm{a}}} + m_o\right) l\sin(\theta) \\ -\left(\frac{m_a}{l_{\mathrm{a}}} + m_o\right) l\sin(\theta) & I + \left(\frac{m_a}{l_{\mathrm{a}}^2} + m_o\right) l^2 \end{bmatrix} \begin{bmatrix} \ddot{x}_{\mathrm{b}} \\ \ddot{\theta} \end{bmatrix} = \begin{bmatrix} F_{\mathrm{b}} \\ \tau \end{bmatrix} + \begin{bmatrix} f_{\mathrm{b}}(\theta, \dot{\theta}) \\ f_{\theta}(\theta) \end{bmatrix} \tag{1}$$

where m_{b}, m_{a}, m_{o} are the masses of the base, the arm, and the object, respectively, assuming the object as a point mass. I is the moment of inertia of the arm with length l and center of mass at $l_{\mathrm{a}} \times l$ from the base of the arm. f_{b} and f_{θ} are state-dependent nonlinear terms. The output, end effector positions in Cartesian space, x_{e} and y_{e}, can be found with:

$$\begin{cases} x_{\mathrm{e}} = x_{\mathrm{b}} + l\cos(\theta) \\ y_{\mathrm{e}} = l\sin(\theta) \end{cases} \tag{2}$$

It is apparent that analytical design of a controller based on the highly nonlinear dynamics in equations (1) and (2) would be difficult. Hence, one can primarily consider the linear part of the dynamics of the manipulated object, written as:

$$\begin{cases} \ddot{x}_{\mathrm{e}} = \frac{F_{\mathrm{e}x}}{m_{\mathrm{o}}} + f_x(\ddot{x}_{\mathrm{b}}, \ddot{\theta}, \dot{\theta}) \\ \ddot{y}_{\mathrm{e}} = \frac{F_{\mathrm{e}y}}{m_{\mathrm{o}}} - g + f_y(\ddot{\theta}, \dot{\theta}) \end{cases} \tag{3}$$

where f_x and f_y are non-linear components of the dynamics, unaccounted for in the Cartesian PD controller design and compensated for in the L1 adaptive controller design. $F_{\mathrm{e}x}$ and $F_{\mathrm{e}y}$ are the resultant forces at the end effector from the locomotion and arm actuation, F_{b} and τ, which affect the object dynamics as the input. Our framework will determine these required resultant forces, broken down into an orthogonal pair in the world x and y direction, making it compatible with Cartesian control. Figure 1 illustrates the simplified model, its degrees of freedom, and the components of resultant force components.

In order to simulate the system, Simscape Multibody – a MATLAB extension that provides full order simulation of dynamics of mechanical components and commonly used in robotics – is used. With customizable geometry, one can easily generate visualization of the results, while feeding corresponding state feedback to the controllers in simulation. A visualization output of our model in Simscape is shown in Figure 1. The actuation inputs are labeled in yellow; the control inputs for the end effector object are labeled in blue.

DOI: 10.54254/2753-8818/14/20240944

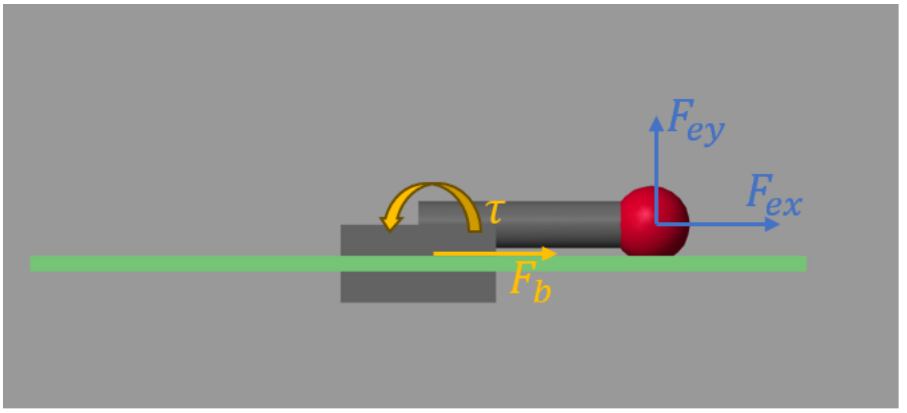

Figure 1. Visualization of the 1 DOF arm mounted on a moving base (photo credit: original).

2.2. Cartesian PD Control

Given the end effector object dynamics in equation (3), one can analytically design a PD controller in Cartesian space using classical control methods to achieve desired performances such as the steady state error, setting time, and maximum overshoot. For the PD control law of

$$F_{\mathrm{e}} = K_{\mathrm{PD}} \begin{bmatrix} r - P_{\mathrm{e}} \\ \dot{r} - \dot{P}_{\mathrm{e}} \end{bmatrix} \tag{4}$$

where r is the end effector position command, $F_{\mathrm{e}} = \begin{bmatrix} F_{ex} \\ F_{\mathrm{e}y} \end{bmatrix}$, and $P_{\mathrm{e}} = \begin{bmatrix} x_{\mathrm{e}} \\ y_{\mathrm{e}} \end{bmatrix}$. One can choose the PD gain matrix to be block diagonal to decouple control inputs on different Cartesian coordinate axis in world frame. In order to map the end effector forces from the Cartesian PD to actuation inputs, define the Jacobian of the end effector positions in Cartesian space with respect to each joint position:

$$J = \frac{\partial P_{\mathrm{e}}}{\partial q} \tag{5}$$

where $q = \begin{bmatrix} x_{\mathrm{b}} \\ \theta \end{bmatrix}$. By matching the work done in joint space and cartesian space, one obtains

$$F_e^T \delta X - \begin{bmatrix} F_{\mathrm{b}} \\ \tau \end{bmatrix}^T \delta q = 0 \tag{6}$$

Substitution the relations in equation (5) into equation (6), one can find the actuation force and torque described in equation (4) with the Jacobian.

$$\begin{bmatrix} F_{\mathrm{b}} \\ \tau \end{bmatrix} = J^T F_{\mathrm{e}} \tag{7}$$

One must note that this actuation mapping assumes static equilibrium of the system, which introduces error at high end effector or joint velocities. This change in the control effectiveness is a matched uncertainty to be accounted for in the L1 adaptive controller.

2.3. L1 Adaptive Controller Design

To mitigate tracking error arising from the model perturbations and nonlinearities in the dynamics of the robot-arm system and the object, L1 adaptive controller is designed such that the uncertainties includes both matched and unmatched uncertainties. The assumptions and derivations of L1 adaptive laws for systems with unmatched uncertainties, along with proofs of transient and steady state performance are explained in chapters 3.2 and 3.3 in [10]. Write the adaptive control problem using the same dynamics representation in Cartesian space, decoupling the linear part of the dynamics in the x and y direction.

DOI: 10.54254/2753-8818/14/20240944

$$\dot{X}(t) = A_m X(t) + B_m\big(\omega u(t) + f_1(X,Z,t)\big) + B_{um} f_2(X,Z,t), X(0) = X_0 \tag{8}$$

$$\dot{Z}(t) = g(X,Z,t)$$

$$y(t) = C_m X(t)$$

In which the measured states $X \triangleq \begin{bmatrix} x_e \\ \dot{x}_e \\ y_e \\ \dot{y}_e \end{bmatrix}$ contains the positions and velocities of the end effector object. ω is the unknown control effectiveness from model perturbations and uncertainties. $g(X,Z,t)$ is an unknown nonlinear function that describes the dynamics of the unmeasured states, such as the joint velocities. To capture effects of unmatched uncertainties on the dynamics, B_{um} is the nullspace of B_m. Let $B \triangleq [B_m\ B_{um}]$ From the problem defined above, define the state predictor:

$$\dot{\hat{X}}(t) = A_m \hat{X}(t) + B_m\big(\omega_0 u(t) + \hat{\sigma}_1(t)\big) + B_{um}\hat{\sigma}_2(t), \hat{X}(0) = \hat{X}_0 \tag{9}$$

$$\hat{y}(t) = C_m \hat{X}(t)$$

where ω_0 is the best guess of ω. State prediction error is defined as $\tilde{X} = \hat{X} - X$. Matrices A_m of $n \times n$, B_m of $n \times m$, and C_m of $m \times n$ must construct a controllable system, while A_m is Hurwitz with desired dynamics that can be analytically designed in linear control. For this system, write:

$$B_m \triangleq \begin{bmatrix} 0 & 0 \\ \hat{m}_o^{-1} & 0 \\ 0 & 0 \\ 0 & \hat{m}_o^{-1} \end{bmatrix} \tag{10}$$

$$C_m \triangleq \begin{bmatrix} 1 & 0 & 0 & 0 \\ 0 & 0 & 1 & 0 \end{bmatrix} \tag{11}$$

$$\omega_0 \triangleq \mathbb{I}_2 \tag{12}$$

In this case, $\hat{m}_o$ is the expected object mass. Define the control law for the input, written in Laplace domain:

$$u(s) = -KD(s)\hat{\eta}(s) \tag{13}$$

where $D(s)$ is a strictly proper transfer function that must satisfy $D(0) = 1$ to achieve asymptotic tracking of the reference states. The feedback gain K can be selected such that $-\omega K$ is Hurwitz among all conservative assumptions of ω. Let:

$$\hat{\eta}(t) \triangleq \omega_0 u(t) + \hat{\eta}_1(t) + \hat{\eta}_{2m}(t) - r_g(t) \tag{14}$$

where $\hat{\eta}_1$ and $\hat{\eta}_{2m}$ takes the same definition as specified in [10]. While the piecewise adaptation law is used.

$$\begin{bmatrix} \hat{\sigma}_1(t) \\ \hat{\sigma}_2(t) \end{bmatrix} = \begin{bmatrix} \hat{\sigma}_1(iT_s) \\ \hat{\sigma}_2(iT_s) \end{bmatrix}, t \in [iT_s, (i+1)T_s) \tag{15}$$

$$\begin{bmatrix} \hat{\sigma}_1(iT_s) \\ \hat{\sigma}_2(iT_s) \end{bmatrix} = -\begin{bmatrix} \mathbb{I}_m & 0 \\ 0 & \mathbb{I}_{n-m} \end{bmatrix} B^{-1}\Phi^{-1}(T_s)\mu(iT_s) \tag{16}$$

Where we find

$$\Phi(T_s) \triangleq A_m^{-1}(\exp(A_m T_s) - \mathbb{I}_n) \tag{17}$$

$$\mu(iT_s) = \exp(A_m T_s)\tilde{X}(iT_s) \tag{18}$$

Define the feedforward term

DOI: 10.54254/2753-8818/14/20240944

$$r_{\mathrm{g}}(s) \triangleq K_{\mathrm{g}}(s)r(s) \tag{19}$$

where $r(s)$ is the Laplace transform of the position commands of the end effector object. One can choose

$$K_{\mathrm{g}} = -\left(CA_m^{-1}B_m\right)^{-1} \tag{20}$$

to achieve the desired decoupling properties, following the intended similar properties in the Cartesian PD controller. The adaptive estimates were calculated using the piecewise-constant adaptive law defined in chapter 3.3 in [10] with a sampling time T_{s}. The adaptive estimates calculated at each sampling time are updated in the control law, while the other components are updated as frequently as each sampling time of the state feedback.

2.4. Integration of L1 Adaptation and Cartesian PD

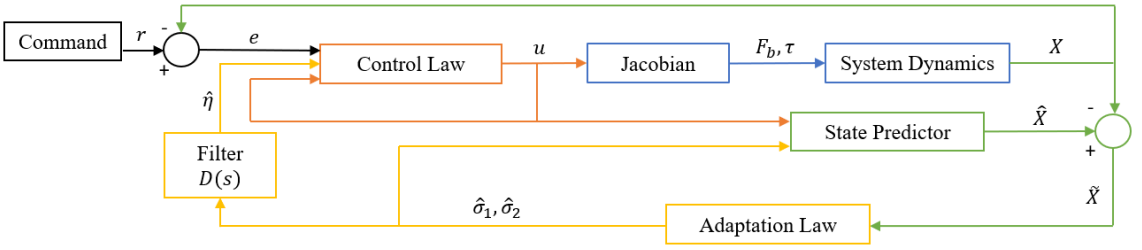

Figure 2. Block diagram of the integrated L1 adaptive Cartesian PD controller. Notice that the control law also involves state error e, in addition to the prediction error $\tilde{X}$ (photo credit: original).

By integrating the Cartesian PD control and L1 adaptive control architecture, this framework retains similar behavior of the Cartesian PD controlled system for end effector tracking, while mitigating the impact of model uncertainties, unmodeled nonlinear dynamics, and external disturbances. The block diagram of the integrated control framework is in Figure 2. In lieu of the feedforward term r_{g} in the control law, this work provides a state feedback term u_{PD} using Cartesian PD control. First, expand the command r with its derivatives:

$$r_{\mathrm{PD}} = \begin{bmatrix} r_1 \\ \dot{r}_1 \\ r_2 \\ \dot{r}_2 \end{bmatrix} \tag{21}$$

The PD control law in equation (4) becomes

$$u_{\mathrm{PD}}(t) = K_{\mathrm{PD}}e(t) \tag{22}$$

where the state error $e \triangleq r_{\mathrm{PD}} - X$. Redefine the input term in equation (14) to accommodate the Cartesian PD control:

$$\hat{\eta}(t) \triangleq \omega_0 u(t) + \hat{\eta}_1(t) + \hat{\eta}_{2m}(t) - r_{\mathrm{g}}(t) \tag{23}$$

The proof of the stability of the closed-loop reference system with the original L1 adaptive controller in the presence of unmatched uncertainties is given in chapter 3.2 of [10]. However, to show the criteria for boundedness of the reference states with Cartesian PD control integrated, one can follow the definition of e to obtain $e_{\mathrm{ref}} = r_{\mathrm{PD}} - X_{\mathrm{ref}}$ for the close-loop reference system. One can conservatively assume

$$\|e\|_{L\infty} < \|r\|_{L\infty} + \left\|x_{\mathrm{ref}_t}\right\|_{L\infty} \tag{24}$$

Similar to the proof in section 3.2.3 in [10], it follows that

DOI: 10.54254/2753-8818/14/20240944

$$(1 - \|H_{xm}(s)C(s)K_{\mathrm{PD}}\|_{L1})\left\|x_{\mathrm{ref}_t}\right\|_{L\infty} \leq \|G_m(s)\|_{L1}\left\|\eta_{1\mathrm{ref}_t}\right\|_{L\infty}$$
$$+\|G_{um}(s)\|_{L1}\left\|\eta_{2\mathrm{ref}_t}\right\|_{L\infty} + \|H_{xm}(s)C(s)K_{\mathrm{PD}}\|_{L1}\|r_{\mathrm{PD}}\|_{L\infty} + \rho_{\mathrm{in}} \quad (25)$$

where one can follow the same definition of $C(s)$, H_{xm}, G_m, G_{um}, and ρ_{in}. With the right-hand side of equation (25) bounded, it can be shown that $\left\|x_{\mathrm{ref}_t}\right\|_{L\infty}$ is bounded given the criteria below:

$$\|H_{xm}(s)C(s)K_{\mathrm{PD}}\|_{L1} < 1 \quad (26)$$

Given the choice of $D(s)$ and K_{PD} in previous sections, one can computationally determine if the criteria in equation (26) is met. Notice that one can adjust A_m, $D(s)$, and K_{PD} to accommodate for the desired object dynamics and the expected bandwidth for disturbances.

3. Simulation Results

For the simplified system of 1 DOF arm on a moving based introduced in Section II, let $m_{\mathrm{b}} = 0.85kg$, $m_{\mathrm{a}} = 0.4kg$, $l = 0.3m$ which is of similar mass to the links of market-available robotic manipulator designs for quadruped robots. I is calculated assuming a cylindrical arm of uniform mass in the simulation; hence, $l_{\mathrm{a}} = 0.5$. The above properties, as well as the actual object mass m_o, are kept unknown in the controller design, with only a range of conservative estimates considered for each parameter. Assume the object mass $\hat{m}_{\mathrm{o}} = 5kg$, which is used in the following controller design:

For the Cartesian PD controller, choose

$$K_{\mathrm{PD}} = \begin{bmatrix} 1000 & 100 & 0 & 0 \\ 0 & 0 & 1000 & 100 \end{bmatrix} \quad (27)$$

For the desired dynamics in the state predictor of the L1 adaptive control, we choose a Hurwitz matrix

$$A_m = \begin{bmatrix} 0 & 1 & & \\ -1 & -1.4 & 0_2 & \\ & & 0 & 1 \\ & 0_2 & -1 & -1.4 \end{bmatrix} \quad (28)$$

The control law gain

$$K = \begin{bmatrix} 50 & 0 \\ 0 & 50 \end{bmatrix} \quad (29)$$

One can design component of the filter

$$D(s) = \frac{1}{s} \quad (30)$$

The sampling time of the piecewise-constant adaptive law

$$T_{\mathrm{s}} = 0.01s$$

while the other components of the framework have sampling times of no greater than 0.001s.

3.1. Effect of L1 Adaptive Control

Initially let $m_{\mathrm{o}} = \hat{m}_{\mathrm{o}}$. Choose K_{g} according to equation (20), such that

$$K_{\mathrm{g}} = \begin{bmatrix} 5 & 0 \\ 0 & 5 \end{bmatrix} \quad (31)$$

Introduce a piecewise ramp command for the end effector to move from its initial location to a specified location in the world frame. The output of the system controlled by the Cartesian PD Controller and the L1 Adaptive Controller is shown in Figure 3.

DOI: 10.54254/2753-8818/14/20240944

$$\begin{cases} r(t) = \begin{bmatrix} 0.3 \\ 0.05 \end{bmatrix} + \begin{bmatrix} 0.25 \\ 0.1 \end{bmatrix} t, & t \leq 2 \\ r(t) = \begin{bmatrix} 0.8 \\ 0.25 \end{bmatrix}, & t > 2 \end{cases} \tag{32}$$

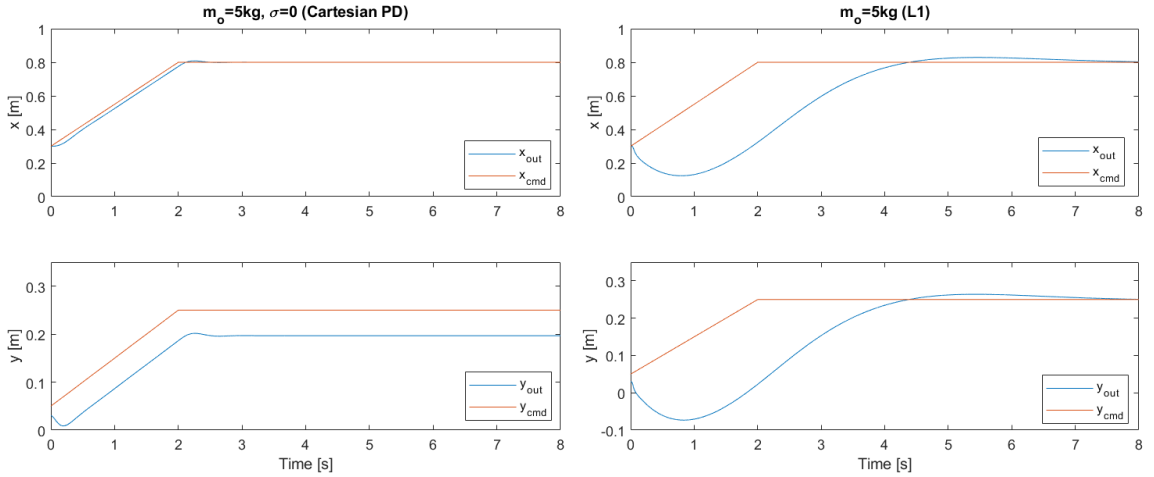

Figure 3. Cartesian PD control (left) resulted in significant steady state error, which was mitigated by L1 adaptive control (right) (photo credit: original).

Although the L1 Adaptive Controller eliminated the steady state error, the transient performance is not desirable and resulted in a greater settling time. Although the controller is proven to have bounded transient error [10], the error was large due to the gravity term of the dynamics being absent from the state predictor dynamics, which was a dominant force of the dynamics in the y position of the object. One must increase the adaptation rate to mitigate this problem; therefore, improvement in transient performance requires much higher gain K, or a redesign of the filter.

3.2. Effect of the Cartesian PD and L1 Adaptation Integration

Using the same example demonstrated in the sub-section above, with the same applicable controller parameters, including identical PD gains, the result of the system with the integrated controller is shown in Figure 4.

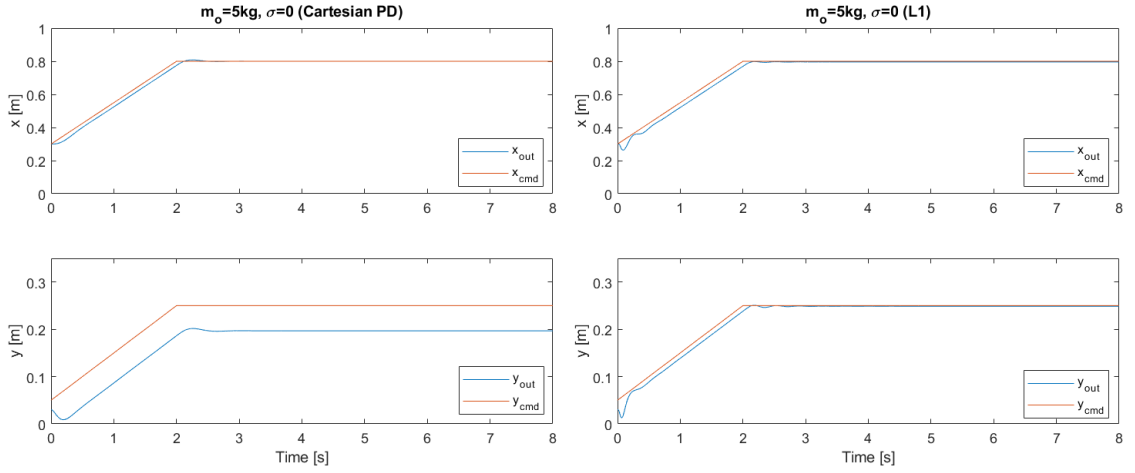

Figure 4. Compared to only the Cartesian PD controller (left), the integrated controller (right) demonstrated superior object state tracking both in transient and steady state performance (photo credit: original).

DOI: 10.54254/2753-8818/14/20240944

The integrated controller showed a similar behavior to the Cartesian PD controller initially, with the error quickly neutralized by the adaptive estimates, fully eliminating the steady state error caused by gravity and nonlinear unmodeled dynamics. The Cartesian PD state feedback term in the input allowed the system to show similar dynamical behavior compared to that of the Cartesian PD controller.

Next, the object mass is perturbed as $m_o = 10kg$, which is twice of the estimated mass. By comparing the results between Figures 4 and 5, the steady state error of the Cartesian PD controlled system grew significantly, along with increased transient error, caused by the higher object mass. Eliminating this additional error would require re-tuning of the controller with an updated mass estimate. With no re-tuning of the integrated controller, the results remained similar to the unperturbed system.

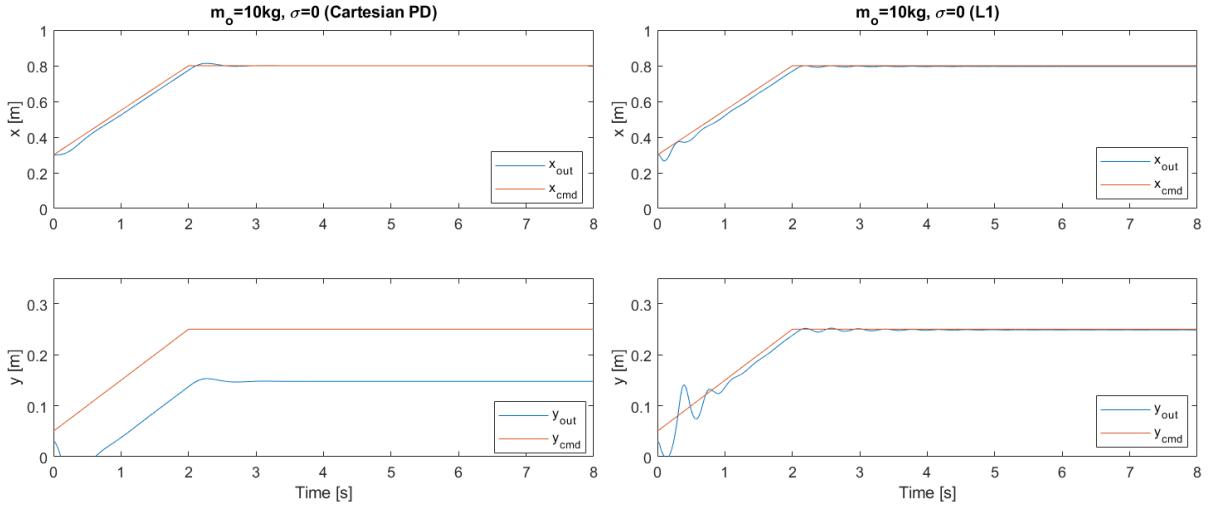

Figure 5. Comparison of the results from the Cartesian PD controller (left) and the integrated controller (right) under a perturbed system (photo credit: original).

In order to investigate the performance and robustness of the integrated controller against disturbances, introduce a horizontal oscillatory external force σ_x of amplitude α and frequency f_σ, applied to the base of the system. Unknown to the controller and non-collocated with any state feedback, this disturbance is a part of the unmatched uncertainties.

To simulate higher frequency and lower magnitude disturbances, such as error from stepping or trotting for locomotion, let $\alpha = 5N$, $f_\sigma = 5s^{-1}$. The results shown in Figure 6 suggests that the integrated controller, with the filter bandwidth for the L1 adaptive controller including the disturbance frequency, is able to eliminate the effects of the disturbance on the output without significant impact on transient performance.

DOI: 10.54254/2753-8818/14/20240944

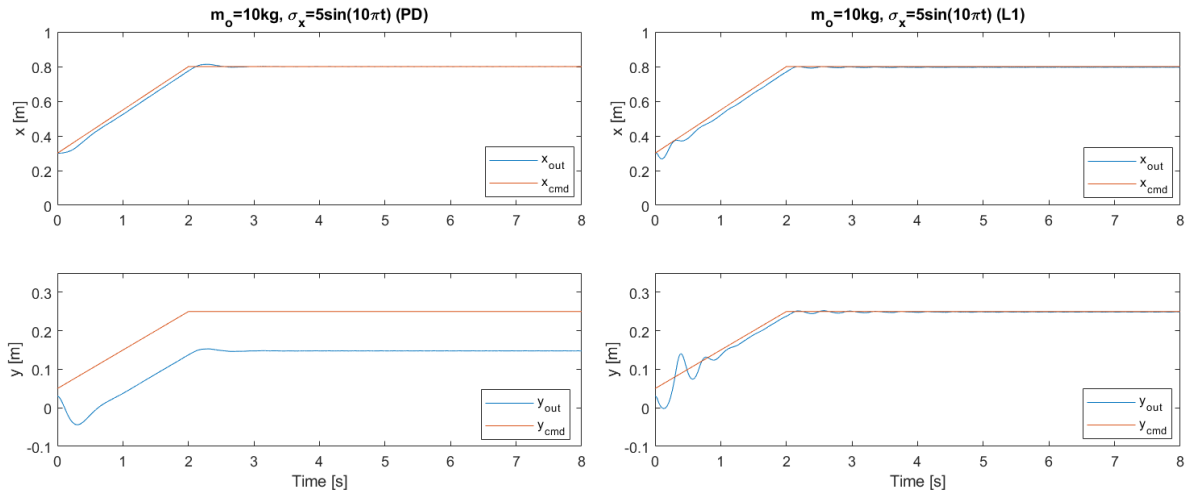

Figure 6. End effector position outputs of the Cartesian PD (left) and integrated (right) controlled systems under higher frequency disturbance (photo credit: original).

Disturbances from external forces on the robot are simulated with a lower frequency and higher amplitude external force applied to the moving base, let $\alpha = 15N$, $f_\sigma = 1s^{-1}$. By comparing the results in Figure 7, one can apparently tell that the Cartesian PD controller exhibited continuing oscillations. In order to reduce the amplitude of the output oscillations, one would need to retune the controller gains, thus altering the transient performance, and potentially the steady-state error, specifically to the expected frequency of the disturbance. The integrated controller, without re-tuning, demonstrated comparable results with those of the undisturbed example, with the effects of the disturbance greatly mitigated. While the feedforward Cartesian PD input gives similar transient behavior to the original Cartesian PD controller, the L1 adaptive component is able to account for non-collocated disturbances as part of the unmatched uncertainties.

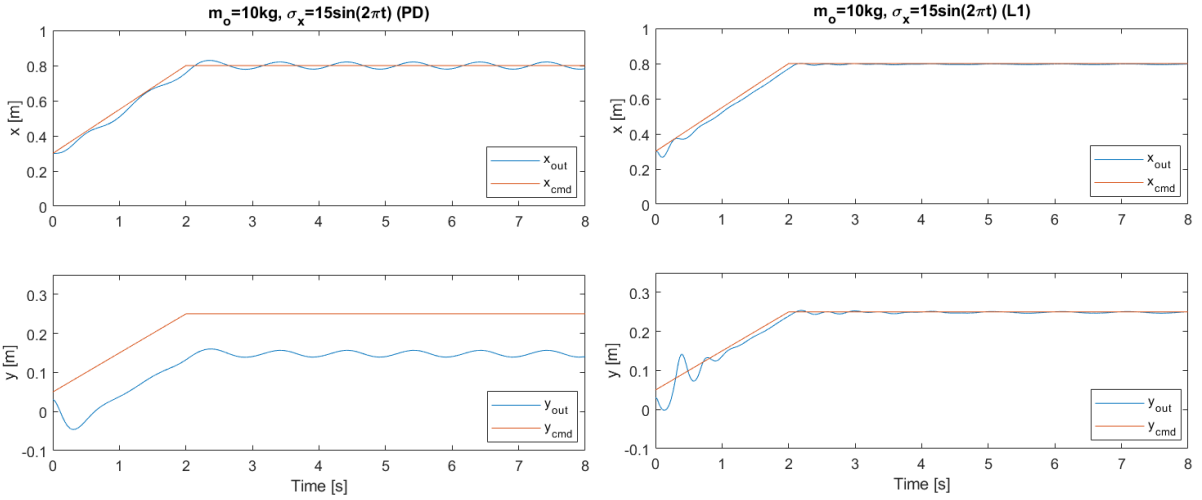

Figure 7. End effector position outputs of the Cartesian PD (left) and integrated (right) controlled systems under lower frequency disturbance (photo credit: original).

4. Conclusion

Through a simplified system of a robotic manipulator arm mounted on a moving base, this work presented a control framework that integrates L1 adaptive control with traditionally used Cartesian PD

DOI: 10.54254/2753-8818/14/20240944

control to track the end effector position. The representation of the dynamics of loco-manipulation by choosing the object states in Cartesian space, especially when manipulating the heavy object, both enabled the linear terms of the dynamics to dominate and the simple characterization of the desired object dynamics in the L1 adaptive controller. This allows the design of the Cartesian PD and L1 adaptive controller mostly separately, with the exception of the stability requirement presented in equation (26). Subsequently, one can choose the desired characteristics of the object dynamics and controller tuning separately, which was shown in the results that the integration of L1 adaptive controller produced output that bears resemblance to that of a Cartesian PD controller imposed on the desired dynamics. Most noticeably, through designing for unmatched uncertainties with conservative estimates, the integrated controller was able to mitigate common model perturbations and external disturbances without re-tuning, demonstrating similar tracking behavior in various cases of uncertainties.

This demonstration of the integrated controller framework shows promise to many further extensions for applications on robot loco-manipulation. By investigating the configuration of current market-available 6 DOF manipulators, one can expand this framework to account for both rotational and translational states of the end effector or object for manipulation. Although this framework only involved PD feedforward input, one can integrate the control law of the L1 adaptive controller with linear optimal control. The relatively low computational cost of the L1 adaptive controller allows quick mitigation of impact of uncertainties, especially from unmodeled nonlinear dynamics, while keeping the advantage of the computational efficiency of linear optimization methods.

References

[1] Di Carlo J, Wensing P M, Katz B, Bledt G and Kim S Dynamic locomotion in the mit cheetah 3 through convex model-predictive control 2018 IEEE/RSJ International Conference on Intelligent Robots and Systems (Madrid) pp 1-9

[2] Jenelten F, Miki T, Vijayan E, Bjelonic M and Hutter M Perceptive locomotion in rough terrain–online foothold optimization 2020 IEEE Robotics and Automation Letters vol 5 no 4 pp 5370-5376

[3] Sombolestan M, Chen Y and Nguyen Q Adaptive force-based control for legged robots 2021 IEEE/RSJ International Conference on Intelligent Robots and Systems (Prague) pp 7440-7447

[4] Sleiman J, Farshidian F, Minniti M V and Hutter M A unified mpc framework for whole-body dynamic locomotion and manipulation 2021 IEEE Robotics and Automation Letters vol 6 no 3 pp 4688 - 4695

[5] Hovakimyan N, Cao C, Kharisov E, Xargay E and Gregory I M L1 adaptive control for safety-critical systems 2011 IEEE Control Systems Magazine vol 31 no 5 pp 54-104

[6] Gregory I M, Xargay E, Cao C and Hovakimyan N Flight test of an L1 adaptive controller on the nasa airstar flight test vehicle 2010 AIAA Guidance, Navigation, and Control Conference (Toronto)

[7] Kharisov E, Hovakimyan N and Åström K J Comparison of several adaptive controllers according to their robustness metrics 2010 AIAA Guidance, Navigation, and Control Conference (Toronto)

[8] Xargay E, Hovakimyan N and Cao C Benchmark problems of adaptive control revisited by L1 adaptive control 2009 17th Mediterranean Conference on Control and Automation (Thessaloniki) pp 31-36

[9] Patel V V, Cao C, Hovakimyan N, Wise K A and Lavretsky E L1 adaptive controller for tailless unstable aircraft in the presence of unknown actuator failures 2009 International Journal of Control vol 82 no 4 pp 705-720

[10] Hovakimyan N and Cao C 2010 L1 Adaptive Control Theory: Guaranteed Robustness with Fast Adaptation (Philadelphia: Society for Industrial and Applied Mathematics) pp 140-177

[11] Nguyen Q and Sreenath K L1 adaptive control for bipedal robots with control lyapunov function based quadratic programs 2015 American Control Conference (Chicago) pp 862-867